

Theoretical modeling of holmium-doped fiber lasers pumped by laser-diodes around 1.15 μm

Fatma Ayad Raghb* , Abdulkareem H. Dagher

Department of Physics, College of Education, University of Mustansiriyah, Baghdad, Iraq.

*Corresponding author: fatmaayad_9610@uomustansiriyah.edu.iq

Original Research

Abstract:

Published online:
15 June 2024

© The Author(s) 2024

At theoretical model of three levels describing Holmium-doped fiber lasers (HDFL) pumped by Laser-diodes 1.15 μm is presented. Based on the model, each of the efficiency, output power depending on fiber core radius, fiber length, and ion concentration of active media were investigated, using the MATLAB program (R 2019 a). The results show that at a doped fiber core radius, 2, 5 & 10 μm pumped with a power range of 10 - 100 W got an output power ranging from 5 to 55 W, respectively, while slope efficiency (η) was 31.3%. Output power was 2.7 - 4 W, $\eta = 50\%$ at a fiber length of 0.01 m, and 81.7 - 83 W, $\eta = 19.6\%$ at a fiber length of 0.5 m. The output power ranged from 107.8 to 109 W & $\eta = 4.7\%$ for 3 m fiber length. The threshold power value of $P_{th} = 0.05$ W at fiber core radius 2 μm and $P_{th} = 0.006$ W at 3 μm was then gradually slightly increased from 4 to 10 μm . As a result, the output power and efficiency are no longer reliant on the diameter of the fiber core.

Keywords: Holmium; V-parameter; Fiber laser; Modeling; Numerical analysis; High out power; Free-space communications

1. Introduction

Strong interest in rare earth-doped fiber lasers research arises from high output power and convenient generators of ultrafast pulses. A particular examples the holmium-doped silica fiber laser, provides an efficient method of generating high average power at 2.1 μm spectral region that is an excellent atmospheric transmission window. It is attractive in applications involving free-space beam propagation, such as atmospheric sensing, free-space communications, and LIDAR [1]. Eye safety is an additional vital consideration in such applications [2]. Holmium-doped fibers have two main pump absorption bands that are located at the central wavelengths of 1.95 μm ($^5\text{I}_8 \rightarrow ^5\text{I}_7$ transition) and 1.15 μm ($^5\text{I}_8 \rightarrow ^5\text{I}_6$ transition). Focusing on output power and efficiency to improve the laser performance, some important parameters such as absorption power P_{abs} , threshold power P_{th} , V-parameter, and effective area A_{eff} were examined with optical fiber core radius.

2. Theoretical model

Assuming a laser system has three energy levels, an ion at a given level can generally transition spontaneously (either radiating or not) to any lower level, or it can be stimulated to emit at a higher or lower level. Fig. 1 depicts the energy levels structure in-band pumped for a holmium-doped fiber laser, showing the two primary transitions: the laser transition (2.1 μm) and the pump transition (1.15 μm).

The rate equations are [4]

$$\frac{dN_3}{dt} = N_1 W_P - N_3 X_P W_P - N_3 W_3 \quad (1)$$

$$\frac{dN_2}{dt} = N_3 W_{32} + N_1 W_{12}^d - N_2 W_2 - N_2 W_{21}^d \quad (2)$$

$$\frac{dN_1}{dt} = N_3 W_{31} + N_2 W_{21}^d + N_2 W_{21} - N_1 W_{12}^d - N_1 W_1 \quad (3)$$

$$N_0 = N_1 + N_{ex} \quad (4)$$

$$N_{ex} = N_2 + N_3 \quad (5)$$

N_0 , N_{ex} & N_i are number of ions per unit volume, population in the excited states and number of ions per unit volume

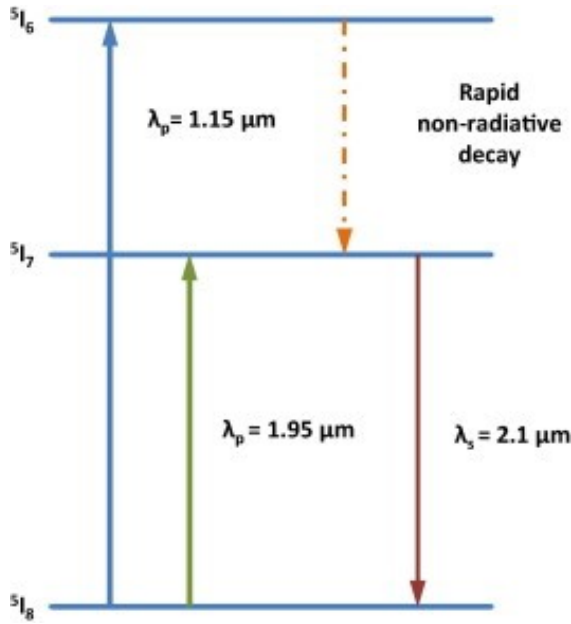


Figure 1. Pumping system commonly used in holmium doped silica [3].

in level i respectively. W_{ij} & W_{ij}^d probability per unit time that an ion in level i decays spontaneously to level j and transition rate from level i to level j induced by stimulated emission or absorption respectively [1].

Equating zero and use branching ratio notations Eq. (1), Eq. (2), Eq. (3) becomes

$$N_3 = R_P \tau_3 \tag{6}$$

$$N_2 = R_P \tau_2 \beta_{32} - \Delta N W_{21}^d \tau_2 \tag{7}$$

$$N_1 = R_P \tau_1 \beta_{31} + \Delta N W_{21}^d \tau_1 (1 - \beta_{21}) \tag{8}$$

where

$$\tau_i = \frac{1}{W_i}, \quad \Delta N = N_2 - X_r N_1$$

$$X_r = \frac{W_{12}^d}{W_{21}^d}, \quad \text{and} \quad R_P \equiv \frac{N_1 W_P}{1 + X_P W_P \tau_3}$$

Population difference is

$$\Delta N = R_P \frac{\tau_a}{1 + W_{32}^d \tau_b} \tag{9}$$

where: $\tau_a = \beta_{32} \tau_2 - X_r \beta_{31} \tau_1$ & $\tau_b = \tau_2 + \tau_1 X_r (1 - \beta_{21})$. Then Eq. (8) become

$$N_1 = N_0 \frac{1 + X_P W_P \tau_3}{1 + W_P (\tau_{ex} + X_P \tau_3)} \tag{10}$$

where: $S = W_{21}^d \tau_b = I/I_{sat}$, $a_2 = 1 - (\tau_2 \tau_a / \tau_b \tau_e)$, $\tau_{ex} = \tau_e (1 + a_2 S) / (1 + S)$, $I_{sat} \equiv h\nu_L / \sigma_L \tau_b$, and $\tau_e = \sum_{i=2}^4 \beta_{4i} \tau_i$, $T \equiv 1 - R_2$, the combination P_P , with P_{out} is: where

$$P_{out} = P_P \frac{\tau_a \sigma_L T S I_{sat} (1 - \gamma)}{2\gamma G_{th} h\nu_P (1 + S)} \tag{11}$$

where

$$\gamma = \exp(-\alpha_P L + a_3 (1 + a_4 S) G_{th} \frac{\sigma_P}{\sigma_L}),$$

$$a_3 \equiv \frac{\tau_e + \tau_P}{\tau_a} \quad \& \quad a_4 = \frac{a_2 \tau_e + \tau_P}{\tau_e + \tau_P}$$

The pumping threshold for CW lasing is [4]:

$$P_{th} = G_{th} \frac{h\nu_P A_{eff}}{\tau_a \sigma_L} \frac{\beta}{(1 - \beta)} \tag{12}$$

that

$$\beta = \exp(-\alpha_P L + a_3 G_{th} \frac{\sigma_P}{\sigma_L})$$

where, $h\nu_P$ is the pump photon energy, G_{th} is the gain at the threshold, A_{eff} is the effective core area of the fiber, and σ_L is the stimulated emission cross section for the $2 \rightarrow 1$ lasing transition.

Characterized by the fact that it depends on the properties of the laser emitting material, such as the effective area of the stimulated emission cross-section and the lifetime of illumination or emission, in addition to the type of signal style. It is also somewhat independent of the pumping pattern as long as this pattern is sufficiently far from the cutoff ($\eta_P \approx 1$). Describes laser efficiency as the ratio of change output power to input power. However, this definition is not very useful in the case of saturation of the output, because the slope efficiency in this case depends on the pumping capacity. Optimized efficiency is defined as the ratio of output power to optimized pumping power. The improved pumping power is the lower input power that is sufficient to obtain the given output power [4]. The laser output gradient efficiency is given by the following formula [5]:

$$\eta_s = \eta_P \frac{T h\nu_L}{\delta h\nu_P} \tag{13}$$

η_P is the percentage of pumping energy contained in the fiber core, T is the transmittance of the output mirror, $h\nu_L/h\nu_P$ is the ratio of laser photon energy to pumping photon energy, this ratio constitutes the limit essential for the efficiency of the process of converting the energy of any photon into another photon. While δ represents total losses of laser intensity for round trip and corresponds to $2G_{th}$ here. The output power of this fiber laser is given in terms of the absorbed pumping power P_{abs} by the relationship:

$$P_{out} = \eta_s (P_{abs} - P_{th}) \tag{14}$$

where $P_{abs} = P_P(0)[1 - \exp(-\alpha_P L)]$ and $P_P(0)$ represents the pumping power at the doped fiber's intake, and the laser output ramp efficiency η_s is a measure of the efficiency with which the doped fiber laser transforms the incident pumping power once it reaches threshold limit to output power. Specifies the kind of optical fiber, single or multi-mode, and be in the range of $1.2 < V > 2.4$ using equation [6]

$$V = \frac{2\pi r}{\lambda} \sqrt{n_1^2 - n_2^2} = \frac{2\pi r}{\lambda} N_A \tag{15}$$

The radius of a single mode is so short that only one mode of light transmission is possible. High bandwidth and low

noise are two good optical features provided by this mode. Radius of a multi-mode is more than large enough to support multiple modes of operation; these offers less effective optical characteristics, like smaller bandwidth and more noise.

3. Results and discussion

All parameters included in the present model for the holmium-doped fiber laser, which was used in simulation to calculate output power P_{out} , efficiency η , standard frequency V , effective area A_{eff} , and threshold power P_{th} are shown in Table 1.

Studying the effect of each parameter on output power separately to obtain the best laser output and efficiency used in several applications. Fig. 2 shows the output power of the holmium fiber laser versus pumping power at different doped fiber core radii (2, 5 & 10) μm . Pump powers of 10 to 100 W gave output powers of 5 to 55 W, respectively, while the ramp efficiency η was 31.3%. Compare this with reference [8] which state that at wavelength 1.25 μm , core radius 10 μm , and pump power (2 - 35) W without excited state absorption, slope efficiency 30% and output power (1 - 17.5) W.

Fig. 3 shows the behavior of output power with various fiber core radiuses for lengths 0.01, 0.5 & 3 m. It seems that, for specific fiber length, there are a few changes in P_{out} for alternating core radius. This result agrees with the score paper [11]. The horizontal lines depict the output power at various fiber lengths; the output power was (2.7 - 4) W, $\eta = 50\%$ at a fiber length of 0.01 m, (81.7 - 83) W, $\eta = 19.6\%$ at fiber length 0.5 m. The output power ranged from (107.8 - 109) W and $\eta = 4.7\%$ for 3 m fiber length. These results are approximately in agreement with Fig. 5 from reference [8] displays the calculated output power as

Table 1. Basic parameters used in the numerical simulations.

Parameters	Value	unit	Reference
τ_2	7.35	(ms)	[7]
τ_3	3.521	(ms)	[7]
λ_p	1.15	(μm)	[8]
σ_p	1.5×10^{-25}	(m^2)	[8]
λ_L	2.1	(μm)	[8]
σ_L	3×10^{-25}	(m^2)	[8]
W_{21}	61.7	s^{-1}	[9]
W_{31}	72.3	s^{-1}	[9]
W_{32}	15.01	s^{-1}	[9]
N_A	0.0681	-	Calculated
n_1	1.448	-	[10]
n_2	1.451	-	[10]

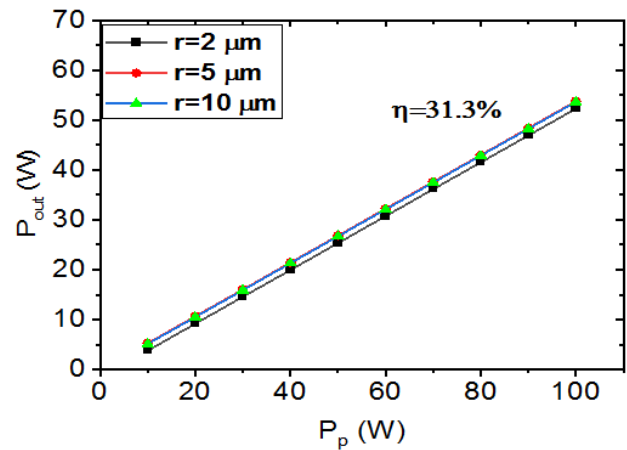


Figure 2. Holmium fiber laser output power against pumping power for various core radii at $N = 4 \times 10^{23} \text{ ion/m}^3$, $L = 0.2 \text{ m}$.

a function of pump power for different lengths. As we can see, output power 11.8 W with a slope efficiency of 33% was achieved when 1.15 m pumping was launched. As the fiber length increased, leading to abundant absorption of the pump power, the maximum slope efficiency of 37% can be obtained when fiber length varies between (0.8 ~ 1.2) m. According to Fig. 4, increasing the concentration of holmium can result in more excited electrons, which raises output power. The output power ranged from 17.7 to 19 W & $\eta = 44.6\%$ at concentration of $1 \times 10^{23} \text{ ion/m}^3$, 59.5 to 60.9 W & $\eta = 28.4\%$ at concentration of $5 \times 10^{23} \text{ ion/m}^3$ and 81.7 to 83 W & $\eta = 19.6\%$ at concentration of $10 \times 10^{23} \text{ ion/m}^3$. The core radius of 2 to 10 μm output power have, approximately the same value for specific ion concentrations. These findings were comparable with the source [11]. A smaller shell diameter improved interference between the pump and the doped nucleus, while a lower holmium concentration lessened the impact of ion aggregation on laser efficiency.

Characteristic of output power, $P_{out} = 52.3 \text{ W}$ at 2 μm and $P_{out} \approx 53.8 \text{ W}$ at (3 & 4) μm then became semi-reduction

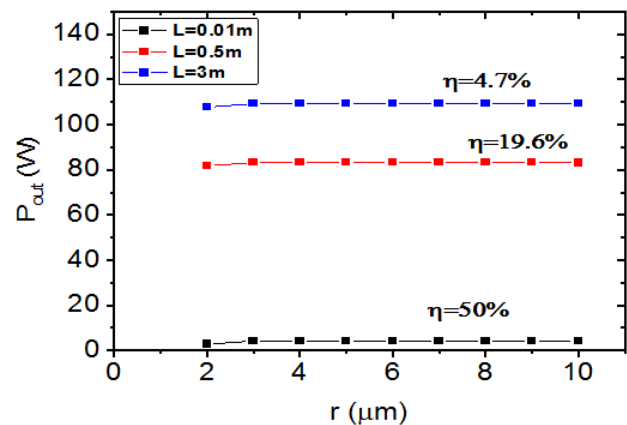


Figure 3. Output power of holmium-doped fiber as a function of fiber core radius with different fiber length at $P_p = 100 \text{ W}$, $N = 4 \times 10^{23} \text{ ion/m}^3$.

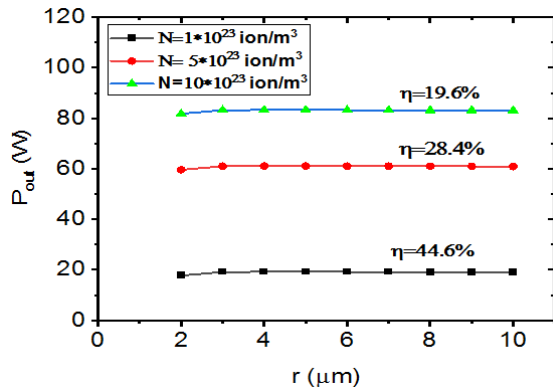


Figure 4. Output power of holmium-doped fiber as a function of fiber core radius with different ion consternation at $P_p = 100\text{ W}$, $L = 0.2\text{ m}$.

for (5 - 10) μm , while threshold power value $P_{th} = 0.05\text{ W}$ at 2 μm and $P_{th} = 0.006\text{ W}$ at fiber core radius 3 μm then gradually slight increased for (4 - 10) μm as in Fig. 5. Surface area interacts with the pump beam rises as the core radius increases, amount of excited electrons boost. Fiber radius expanded, more light travels through the fiber, leading to photons being lost before they have a chance to activate electrons.

V parameter determines the number of modes supported by a fiber and cut-off condition of various modes, the fundamental mode has no cut-off and always propped by a fiber. Fig. 6 shows that the value of standard frequency V was increased linearly with radius, determining the type of fiber. The standard frequency is the frequency of light that travels in optical fibers without dispersion, which increases constantly as the radius increases, which is based on the optical fiber's radius and the fiber manufacturing material's refractive index. The fiber effective area $A_{eff} = \pi w^2$ represents the cross-sectional area of the fiber over which light efficiently propagated. Fig. 6 curve shows the extent of light confinement in the core of fiber, so the concluded radius does not affect the effective area of holmium fibers where the fiber core is single-mode or multi-mode. The effective fiber area for the holmium fibers is quite small, equaling $(0.027 - 0.15) \cdot 10^{-8}\text{ m}^2$. This means that regardless of the

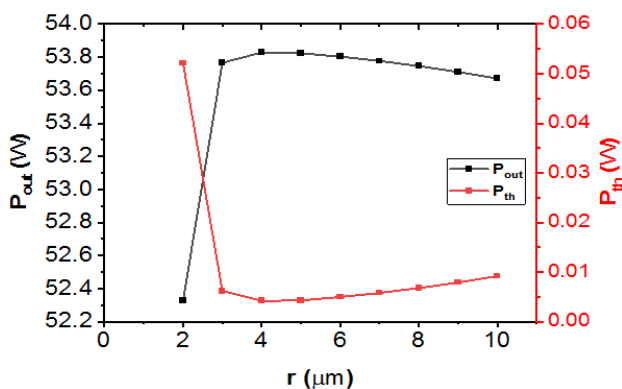


Figure 5. Output and threshold power as a function of core radius, at $P_p = 100\text{ W}$, $N = 4 \times 10^{23}\text{ ion/m}^3$, $L = 0.2\text{ m}$.

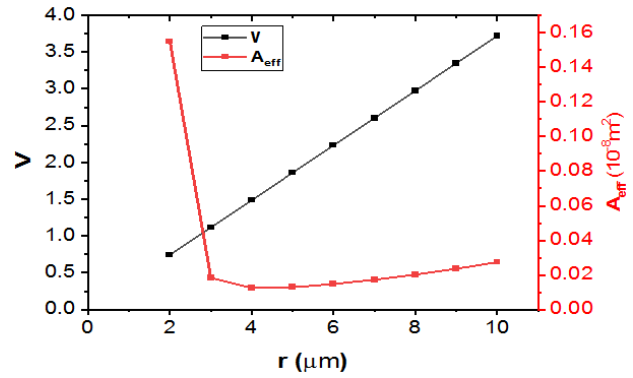


Figure 6. The fiber's effective core cross-sectional area and standard frequency function of core radius.

radius of the fiber core and the light in the holmium fiber is constrained to a relatively narrow area.

4. Conclusion

In the present work, the operation of output power and efficiency were investigated for several parameters of HDFL under theoretical study. Lengthening the fiber or increasing the concentration of holmium inside the fiber, electrons that are more excited can be produced, bringing about altitude P_{out} & diminishing η . Output power and efficiency are no longer available, relying on the diameter of fiber core. This investigation is useful for the design of LD directly pumped Ho-doped lasers, especially high-power lasers. It will be useful to design more efficient Ho-doped fibers for high-power laser sources emitting at $\lambda = 2.1\ \mu\text{m}$. Agreement of our simulation with the result of other papers shows that it provides a good understanding of the laser system.

Authors Contributions

Authors have contributed equally in preparing and writing the manuscript.

Availability of data and materials

Data presented in the manuscript are available via request.

Conflict of Interests

The author declare that they have no known competing financial interests or personal relationships that could have appeared to influence the work reported in this paper.

Open Access

This article is licensed under a Creative Commons Attribution 4.0 International License, which permits use, sharing, adaptation, distribution and reproduction in any medium or format, as long as you give appropriate credit to the original author(s) and the source, provide a link to the Creative Commons license, and indicate if changes were

made. The images or other third party material in this article are included in the article's Creative Commons license, unless indicated otherwise in a credit line to the material. If material is not included in the article's Creative Commons license and your intended use is not permitted by statutory regulation or exceeds the permitted use, you will need to obtain permission directly from the OICC Press publisher. To view a copy of this license, visit <https://creativecommons.org/licenses/by/4.0>.

- [10] C. Z. Tan. "Determination of refractive index of silica glass for infrared wavelengths by IR spectroscopy.". *J. Non. Cryst. Solids.*, **223**:158–163, 1998. DOI: [https://doi.org/10.1016/S0022-3093\(97\)00438-9](https://doi.org/10.1016/S0022-3093(97)00438-9).
- [11] B. Beaumont, P. Bourdon, A. Barnini, L. Kervella, T. Robin, and J. Le Gouet. "High Efficiency Holmium-Doped Triple-Clad Fiber Laser at 2120 nm.". *J. Light. Technol.*, **40**:6480–6485, 2022. DOI: <https://doi.org/10.1109/JLT.2022.3196807>.

References

- [1] W. Shi, Q. Fang, X. Zhu, R. A. Norwood, and N. Peyghambarian. "Fiber lasers and their applications.". *Appl. Opt.*, **53**:6554, 2014. DOI: <https://doi.org/10.1364/AO.53.006554>.
- [2] A. T. Gursel. "Fiber lasers and their medical applications.". *Opt. Amplifiers-A Few Differ. Dimens.*, , 2018. DOI: <https://doi.org/10.5772/intechopen.76610>.
- [3] N. Simakov, Z. Li, Y. Jung, J. M. O. Daniel, P. Barua, P. C. Shardlow, S. Liang, J. K. Sahu, A. Hemming, W. A. Clarkson, S.-U. Alam, and D. J. Richardson. "High gain holmium-doped fibre amplifiers.". *Opt. Express.*, **24**:13946, 2016. DOI: <https://doi.org/10.1364/OE.24.013946>.
- [4] R. S. Quimby. "Output saturation in fiber lasers.". *Appl. Opt.*, **29**:1268, 1990. DOI: <https://doi.org/10.1364/ao.29.001268>.
- [5] M. J. F. Digonnet and C. J. Gaeta. "Theoretical analysis of optical fiber laser amplifiers and oscillators.". *Appl. Opt.*, **24**:333, 1985. DOI: <https://doi.org/10.1364/ao.24.000333>.
- [6] P. Knight. "Fundamentals of photonics.". *J. Mod. Opt.*, **39**:1400, 1992. DOI: <https://doi.org/10.1080/713823546>.
- [7] J. Wang, D. Il Yeom, N. Simakov, A. Hemming, A. Carter, S. B. Lee, and K. Lee. "Numerical modeling of in-band pumped ho-doped silica fiber lasers.". *J. Light. Technol.*, **36**:5863–5880, 2018. DOI: <https://doi.org/10.1109/JLT.2018.2877817>.
- [8] C. Huang, Y. Tang, S. Wang, R. Zhang, J. Zheng, and J. Xu. "Theoretical modeling of ho-doped fiber lasers pumped by laser-diodes around 1125 μm .". *J. Light. Technol.*, **30**:3235–3240, 2012. DOI: <https://doi.org/10.1109/JLT.2012.2211568>.
- [9] B. Peng and T. Izumitani. "Optical properties, fluorescence mechanisms and energy transfer in Tm^{3+} , Ho^{3+} and Tm^{3+} - Ho^{3+} doped near-infrared laser glasses, sensitized by Yb^{3+} .". *Opt. Mater. (Amst)*, **4**:797–810, 1995. DOI: [https://doi.org/10.1016/0925-3467\(95\)00032-1](https://doi.org/10.1016/0925-3467(95)00032-1).